

# TRANSVERSE BEAM EMITTANCE MEASUREMENTS OF A 16 MeV LINAC AT THE IDAHO ACCELERATOR CENTER

S. Setiniyaz\*, K. Chouffani, T. Forest, and Y. Kim  
Idaho State University, Pocatello, ID, 83209, USA  
A. Freyberger, Jefferson Lab, Newport News, Virginia, 23606, USA

## Abstract

A beam emittance measurement of a 16 MeV S-band High Repetition Rate Linac (HRRL) was performed at Idaho State University's Idaho Accelerator Center (IAC). The HRRL linac structure was upgraded beyond the capabilities of a typical medical linac so it can achieve a repetition rate of 1 kHz. Measurements of the HRRL transverse beam emittance are underway that will be used to optimize the production of positrons using HRRL's intense electron beam on a tungsten converter. In this paper, we describe a beam imaging system using an OTR screen and a digital CCD camera, a MATLAB tool to extract beamsize and emittance, detailed measurement procedures, and the results of measured transverse emittances for an arbitrary beam energy.

## INTRODUCTION

The HRRL is an S-band electron linac located in the beam lab of the Physics Department at Idaho State University (ISU). The HRRL accelerates electrons to energies between 3 and 16 MeV with a maximum repetition rate of 1 kHz. The HRRL beamline has recently been reconfigured to generate and collect positrons.

An Optical Transition Radiation (OTR) based viewer was installed to allow measurements at the high electron currents available using the HRRL. The visible light from the OTR based viewer is produced when a relativistic electron beam crosses the boundary of two mediums with different dielectric constants. When the electron beam intersects the OTR target at a  $45^\circ$  angle, visible radiation is emitted at an angle of  $90^\circ$  with respect to the incident beam direction [1]. These backward-emitted photons are observed using a digital camera and can be used to measure the shape and intensity of the beam based on the OTR image distribution.

Emittance is a key parameter in accelerator physics that is used to quantify the quality of an electron beam produced by an accelerator. An emittance measurement can be performed in a several ways [2, 3]. This work used the Quadrupole scanning method [4] to measure emittance, Twiss parameters, and the beam energy.

## THE EXPERIMENT

### Quadrupole Scanning Method

As shown in Fig. 1 illustrates the basic components used to measure the emittance with the quadrupole scanning method. A quadrupole is positioned at the exit of the linac to focus or de-focus the beam as observed on a downstream view screen. The quadrupole and the screen are located far away to minimize chromatic effects and the veracity of the thin lens approximation used to calculate beam optics. Assuming the thin lens approximation,  $\sqrt{k_1}L \ll 1$ , is sat-

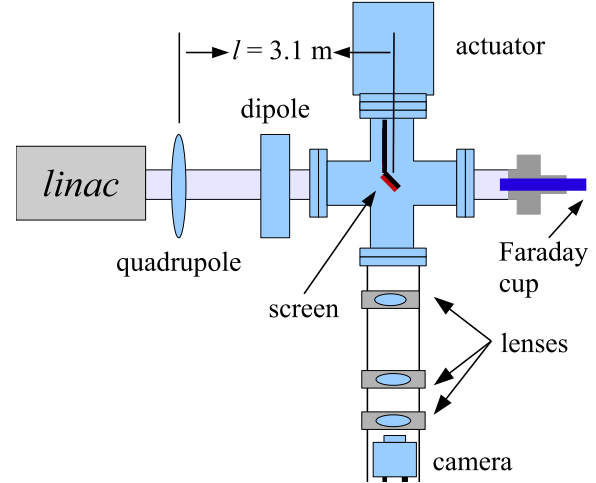


Figure 1: Apparatus used to measure the beam emittance.

isfied, the transfer matrix of a quadrupole magnet may be expressed as

$$\mathbf{Q} = \begin{pmatrix} 1 & 0 \\ -k_1 L & 1 \end{pmatrix} = \begin{pmatrix} 1 & 0 \\ -\frac{1}{f} & 1 \end{pmatrix} \quad (1)$$

where  $k_1$  is the quadrupole strength,  $L$  is the length of quadrupole, and  $f$  is the focal length. A matrix representing the drift space between quadrupole and screen is given by

$$\mathbf{S} = \begin{pmatrix} 1 & l \\ 0 & 1 \end{pmatrix} \quad (2)$$

where  $l$  is the distance between the scanning quadrupole and the screen. The transfer matrix of the scanning region is given by the matrix product  $\mathbf{M}\mathbf{Q}$ . In the horizontal plane, the beam matrix at the screen ( $\sigma_s$ ) is related to the beam

\*Email: sadik82@gmail.com

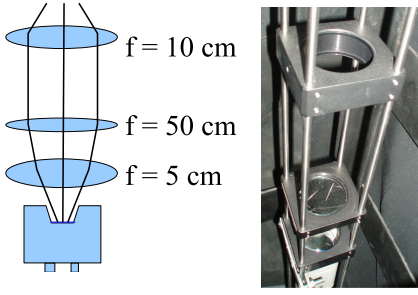


Figure 2: The OTR Imaging system.

matrix of the quadrupole ( $\sigma_q$ ) using the similarity transformation

$$\sigma_s = M\sigma_q M^T \quad (3)$$

where the  $\sigma_s$  is defined as [5]

$$\sigma_{s,x} = \begin{pmatrix} \sigma_{s,x}^2 & \sigma_{s,xx'} \\ \sigma_{s,xx'} & \sigma_{s,x'}^2 \end{pmatrix}, \quad \sigma_{q,x} = \begin{pmatrix} \sigma_{q,x}^2 & \sigma_{q,xx'} \\ \sigma_{q,xx'} & \sigma_{q,x'}^2 \end{pmatrix}. \quad (4)$$

By defining the new parameters [4],

$$A \equiv \sigma_{11}, \quad B \equiv \frac{\sigma_{12}}{\sigma_{11}}, \quad C \equiv \frac{\epsilon_x^2}{\sigma_{11}} \quad (5)$$

the matrix element will describe the square of the beam size at the screen. As a result,  $\sigma_{s,x}^2$  becomes a parabolic function of the product of  $k_1$  and  $L$

$$\sigma_{s,x}^2 = A(k_1 L)^2 - 2AB(k_1 L) + (C + AB^2) \quad (6)$$

The emittance measurement was performed by changing the quadrupole current,  $k_1 L$ , and measuring the corresponding beam image on the view screen. The measured two-dimensional beam image was projected along the images abscissa and ordinate axes. A Gaussian fitting function is used on each projection to determine the rms value,  $\sigma_{s,x}$  in Eq. (6), of the image along each axis. Measurements of  $\sigma_{s,x}$  for several quadrupole current ( $k_1 L$ ) is then fit using the parabolic function in Eq. (6) to determine the constants  $A$ ,  $B$ , and  $C$ . The emittance ( $\epsilon$ ) and the Twiss parameters ( $\alpha$  and  $\beta$ ) can be found using Eq. (7).

$$\epsilon = \sqrt{AC}, \quad \beta = \sqrt{\frac{A}{C}}, \quad \alpha = -B\sqrt{\frac{A}{C}} \quad (7)$$

### The OTR Imaging System

The OTR target is 10  $\mu\text{m}$  thick aluminum foil with a 1.25 inch of diameter. The OTR is emitted in a cone shape with the maximum intensity at an angle  $1/\gamma$  with respect to the reflecting angle of the electron beam [1]. Three lenses, 2 inches in diameter, are used for the imaging system to avoid optical distortion at lower electron energies. Focal lengths and position of the lenses are shown in Fig. 2. The camera used was a JAI CV-A10GE digital camera with 767 by 576 pixel area. The camera images were taken by triggering the camera during synchronously with the electron gun.

### Quadrupole Scanning

The current for one of the beam line quadrupoles is changed to alter the strength and direction of the quadrupole magnetic field such that a measurable change in the beam shape is seen by the OTR system. Initially, the beam was steered by the quadrupole indicating that the beam was not entering along the quadrupoles central axis. Several magnetic elements upstream of this quadrupole were adjusted to align the incident electron beam with the quadrupoles central axis. First, the beam current observed by a Faraday cup located at the end of beam line was maximized using upstream steering coils within the linac nearest the gun. Second, the first solenoid nearest the linac gun was used to focus the electron beam on the OTR screen. Steering coils were adjusted to maximum the beam current to the FC and minimize the deflection of the beam by the solenoid first then by the quadrupole. A second solenoid and the last steering magnet, both near the exit of the linac, were used in the final step to optimize the beam spot size on the OTR target and maximize the Faraday cup current. A configuration was found that minimized the electron beam deflection when the quadrupole current was altered during the emittance measurements.

The emittance measurement was performed using an electron beam energy of approximately 14 MeV and a 40 mA macro pulse peak current. The current in the first quadrupole after the exit of the linac was changed from -5 A to 5 A with an increment of 0.2 A. Seven measurements were taken at each current step in order to determine the average beam width and the variance. Background measurements were taken by turning the linac's electron gun off while keep the RF on. Background image and beam images before and after background subtraction are shown in Fig. 3. A small dark current is visible in Fig. 3b that is known to be generated when electrons are pulled off the cavity wall and accelerated.

The electron beam energy was measured using a dipole magnet downstream of the quadrupole used for the emittance measurements. Prior to energizing the dipole, the single electron bunch charge passing through the dipole was measured using a Faraday cup located approximately 50 cm downstream. The dipole current was adjusted until a maximum single electron bunch charge was observed on another Faraday cup located just after the 45 degree exit port of the dipole. A magnetic field map of the dipole suggests that the electron beam energy was approximately 14 MeV. Future emittance measurements are planned to cover the entire energy range of the linac.

### Data Analysis and Results

Images from the JAI camera were calibrated using the OTR target frame. An LED was used to illuminate the OTR aluminum frame that has a known inner diameter of 31.75 mm. Image processing software was used to inscribe a circle on the image to measure the circular OTR inner frame in units of pixels. The scaling factor can be obtained by dividing this length with the number of pix-

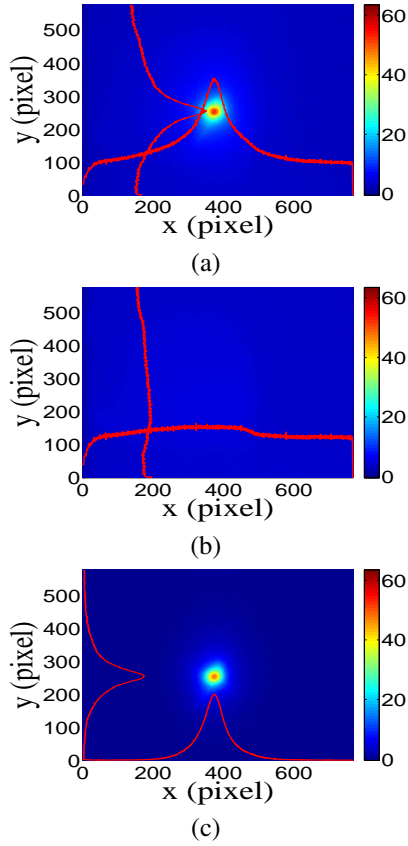


Figure 3: Background subtracted to minimize impact of dark current; (a) a beam with the dark current and background noise, (b) a background image, (c) a beam image when dark background was subtracted.

els observed. The result is a horizontal scaling factor is  $0.04327 \pm 0.00016$  mm/pixel and vertical scaling factor is  $0.04204 \pm 0.00018$  mm/pixel.

Digital images from the JAI camera were extracted in a matrix format in order to take projections on both axes and perform a multi-gaussian or Lorentzian fit. The observed image profiles were not well described by a single Gaussian distribution. The profiles may be described using a Lorentzian distribution, however, the rms of the Lorentzian function is not defined. The super Gaussian distribution seems to be the best option [6] because rms values may be directly extracted.

Fig. 4 shows the square of the rms ( $\sigma^2$ ) vs  $k_1 L$  for  $x$  (horizontal) and  $y$  (vertical) beam projections along with the parabolic fits using Equation 9. The emittances and Twiss parameters from these fits are summarized in Table. 1. Further details describing the fitting procedures are described in reference [7].

## CONCLUSIONS

A diagnostic tool was developed and used to measure the beam emittance of the High Rep Rate Linac at the Idaho Accelerator Center. The tool relied on measuring

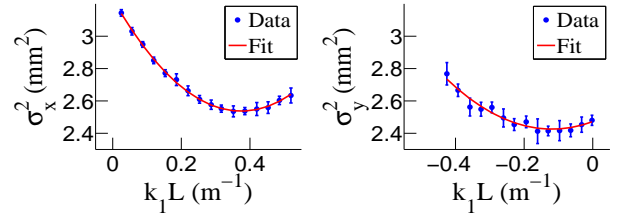


Figure 4: Square of rms values and parabolic fittings.

Table 1: Emittance Measurement Results.

| Parameter                             | Unit          | Value            |
|---------------------------------------|---------------|------------------|
| projected emittance $\epsilon_x$      | $\mu\text{m}$ | $0.37 \pm 0.02$  |
| projected emittance $\epsilon_y$      | $\mu\text{m}$ | $0.30 \pm 0.04$  |
| normalized emittance $\epsilon_{n,x}$ | $\mu\text{m}$ | $10.10 \pm 0.51$ |
| normalized emittance $\epsilon_{n,y}$ | $\mu\text{m}$ | $8.06 \pm 1.1$   |
| $\beta_x$ -function                   | m             | $1.40 \pm 0.06$  |
| $\beta_y$ -function                   | m             | $1.17 \pm 0.13$  |
| $\alpha_x$ -function                  | rad           | $0.97 \pm 0.06$  |
| $\alpha_y$ -function                  | rad           | $0.24 \pm 0.07$  |
| single bunch charge                   | pC            | 11               |
| energy of the beam $E$                | MeV           | 14               |

the images generated by the optical transition radiation of the electron beam on a polished thin aluminum target. The electron beam profile was not described well using a single Gaussian distribution but rather a super Gaussian or Lorentzian distribution. The system appears to more accurately measure the beam's horizontal size because of the larger dynamic range of the imaging system's pixels. The normalized emittance of the High Rep Rate Linac, similar to medical linacs, at ISU was measured to be less than  $10 \mu\text{m}$  when accelerating electrons to an energy of 14 MeV as measured by the OTR based tool described above.

## ACKNOWLEDGMENT

Thanks to C. F. Eckman, C. O'Neill, and Dr. D. Wells.

## REFERENCES

- [1] B. Gitter, Tech. Rep., Los Angeles, USA (1992).
- [2] K.T. McDonald and D.P. Russell, Fron. of Par. Beams Obser. Diag. and Cor. **08544**, (1988).
- [3] Y. Kim *et al.*, in *Proc. FEL2008*, Gyeongju, Korea.
- [4] D.F.G. Benedetti, *et al.*, Tech. Rep., DAFNE Tech. Not., Frascati, Italy (2005).
- [5] S.Y. Lee, *Accelerator Physics*, (Singapore: World Scientific, 2004), 61.
- [6] F.J. Decker, NASA STI/Recon Tech. Rep. N **1996**, (1994) 10487.
- [7] C.F. Eckman *et al.*, in *Proc. IPAC2012*, New Orleans, USA.